

Monte Carlo calculations of Curie temperatures of $Y_{1-x}Gd_x(Fe_{1-y}Co_y)_2$ pseudobinary system

Bartosz Wasilewski^{a,b,c}, Mirosław Werwiński^{a,*}

^a*Institute of Molecular Physics, Polish Academy of Sciences, M. Smoluchowskiego 17, 60-179 Poznań, Poland*

^b*Institute of Mathematics, University of Szczecin, Wielkopolska 15, 70-451 Szczecin, Poland*

^c*Institute of Mathematics, University of Szczecin, Doctoral School, Mickiewicza 16, 70-383 Szczecin, Poland*

Abstract

The close-packed AB_2 structures called Laves phases constitute the largest group of intermetallic compounds. In this paper we computationally investigated the pseudo-binary Laves phase system $Y_{1-x}Gd_x(Fe_{1-y}Co_y)_2$ spanning between the YFe_2 , YCo_2 , $GdFe_2$, and $GdCo_2$ vertices. While the vast majority of the $Y_{1-x}Gd_x(Fe_{1-y}Co_y)_2$ phase diagram is the ferrimagnetic phase, YCo_2 along with a narrow range of concentrations around it is the paramagnetic phase. We presented results obtained by Monte Carlo simulations of the Heisenberg model with parameters derived from first-principles calculations. For calculations we used the Uppsala atomistic spin dynamics (UppASD) code together with the spin-polarized relativistic Korringa-Kohn-Rostoker (SPR-KKR) code. From first principles we calculated the magnetic moments and exchange integrals for the considered pseudo-binary system, together with spin-polarized densities of states for boundary compositions. Furthermore, we showed how the compensation point with the effective zero total moment depends on the concentration in the considered ferrimagnetic phases. However, the main result of our study was the determination of the Curie temperature dependence for the system $Y_{1-x}Gd_x(Fe_{1-y}Co_y)_2$. Except for the paramagnetic region around YCo_2 , the predicted temperatures were in good qualitative and quantitative agreement with experimental results, which confirmed the ability of the method to predict magnetic transition temperatures for systems containing up to three different magnetic elements (Fe, Co, and Gd) simultaneously. For the $Y(Fe_{1-y}Co_y)_2$ and $Gd(Fe_{1-y}Co_y)_2$ systems our calculations matched the experimentally-confirmed Slater-Pauling-like behavior of T_C dependence on the Co concentration. For the $Y_{1-x}Gd_xFe_2$ system we obtained, also in agreement with the experiment, a linear dependence of T_C on the Gd concentration. In addition, on the example of $Y_{0.8}Gd_{0.2}Co_2$ ferrimagnet, we showed the possibility of predicting the non-trivial behavior of the temperature dependence of magnetization, confirmed by comparison with previous measurement results.

1. Introduction

The largest group of intermetallic compounds are the Laves phases [1]. They are binary close-packed structures with a formula AB_2 , which are found in three different types - hexagonal $MgZn_2$ -type (C14), cubic $MgCu_2$ -type (C15), and hexagonal $MgNi_2$ -type (C36), see Fig. 1. In this work, we study theoretically the pseudo-binary cubic Laves phase $Y_{1-x}Gd_x(Fe_{1-y}Co_y)_2$. Its boundary cases are quite well known. $GdFe_2$ and $GdCo_2$ are ferrimagnets with Curie temperature (T_C) equal to 805 K [2] and 390 K [3], respectively. YFe_2 is a ferromagnet with Curie temperature equal to 545 K [2] and YCo_2 is an exchange-enhanced Pauli paramagnet [4] that undergoes a metamagnetic transition in a field of 70 T at 10 K [5, 6]. In Fig. 2 we present a summary of the experimental Curie temperature – concentration relationships for all boundary concentrations [2, 3, 7–9]. We expect the $Y_{1-x}Gd_x(Fe_{1-y}Co_y)_2$

system to be paramagnetic (PM) in the vicinity of YCo_2 , and a little further away to have T_C close to room temperature, see the dotted line. Alloying YCo_2 with either Fe or Gd induces a paramagnetic-ferromagnetic transition at relatively low critical concentrations.

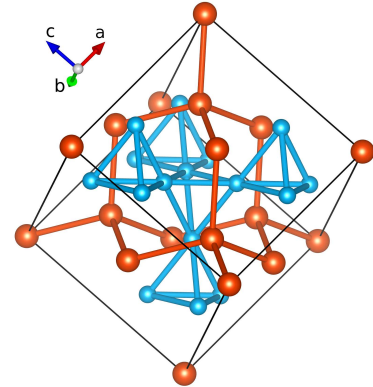


Figure 1: Crystal structure of YCo_2 – cubic $MgCu_2$ -type Laves phase. Y atoms are shown in red, Co atoms in blue.

*Corresponding author

Email address: werwinski@ifmpan.poznan.pl (Mirosław Werwiński)

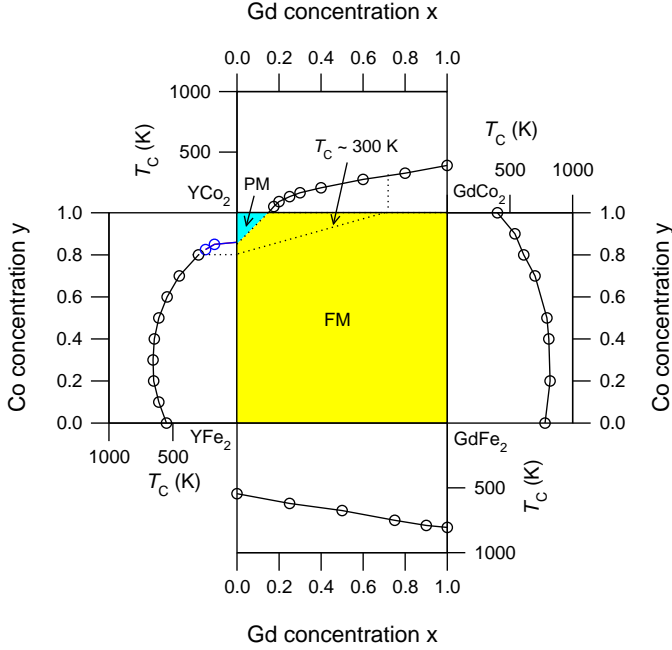


Figure 2: $Y_{1-x}Gd_x(Fe_{1-y}Co_y)_2$ phase diagram deduced from experimental Curie temperatures of boundary concentrations [2, 3, 7–9].

YFe_2 has been identified as a hydrogen storage material [6, 10, 11]. YCo_2 and its alloys have been considered for permanent magnet applications [12]. For the system $Y_{1-x}Gd_xCo_2$, the magnetocaloric [13], thermopower [14], and electronic transport [15] properties have been examined. For the system $Y(Fe_{1-y}Co_y)_2$, electrical resistivity and Mössbauer effect have been investigated [7]. Moreover, rare-earth compounds with large localized magnetic moment, such as Gd, Tb or Er, are some of the most promising candidates for magnetic cooling among Laves phases [16].

Our previous experimental and theoretical studies on the $Y_{1-x}Gd_x(Fe_{1-y}Co_y)_2$ system have included such topics as: effect of YCo_2 doping [17], magnetocaloric effects in $Y_{1-x}Gd_xCo_2$ [13], Curie temperature of $Y(Fe_{1-y}Co_y)_2$ [18], structural disorder in YCo_2 [19], and electronic specific heat coefficient of $Y(Fe_{1-y}Co_y)_2$ [20]. In this work we show the Curie temperatures determined from first principles for pseudo-binary Laves phases $Y_{1-x}Gd_x(Fe_{1-y}Co_y)_2$. The two-site chemical disorder is modeled using Monte Carlo (MC) simulations. The T_C 's are obtained by fashioning the Heisenberg model Hamiltonian with MC simulations using parameters from first-principles calculations. We study the dependence of the exchange integrals on the interatomic distance and analyze the behavior of the total and partial magnetic moments calculated from first principles. We also investigate the valence bands of the stoichiometric boundary compositions. Furthermore, the MC method also allows us to predict the temperature dependence of magnetization (M) and magnetic susceptibility (χ). T_C calculations were performed

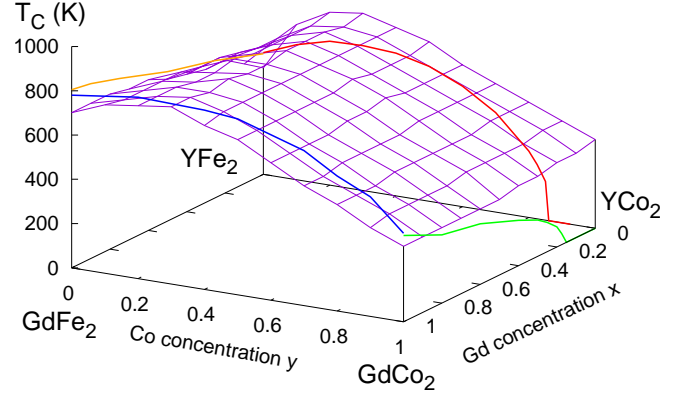


Figure 3: (Purple mesh) Curie temperature dependence of Gd and Co concentrations for $Y_{1-x}Gd_x(Fe_{1-y}Co_y)_2$ determined from Monte Carlo simulations with parameters from the SPR-KKR code. For comparison, the four curves (red, green, blue, and yellow) plotted using experimental results from Refs. [2, 3, 7–9].

for systems containing up to four different elements simultaneously, including three magnetic elements. Although we have previously presented T_C dependence on concentration, e.g. for $Y(Fe_{1-y}Co_y)_2$ [18], in this work for the first time our calculations are based fully on MC simulations and not on the disordered local moment method as before.

2. Calculations' details

One method for determining the Curie temperature is Monte Carlo simulations of the Heisenberg model. The simulations allow to determine the temperature dependence of magnetization and magnetic susceptibility. The location of the peak in magnetic susceptibility allows us to determine T_C with an accuracy of ± 10 K. We obtained the values of the magnetic moments and the exchange integrals necessary to perform the MC simulations from first-principles calculations utilizing the spin polarized relativistic Korringa-Kohn-Rostoker (SPR-KKR) code, version 7.7 [21, 22]. We used the generalized gradient approximation (GGA) in the Perdew, Burke, and Ernzerhof parametrization [23] and the atomic-sphere approximation (ASA) in the fully-relativistic approach. We used the coherent potential approximation (CPA) [24] to simulate chemical disorder. We used the basis functions up to $l = 4$, a $45 \times 45 \times 45$ \mathbf{k} -mesh, and 40 energy points. Exchange integrals were obtained using the method of Liechtenstein *et al.* [25] with respect to the ferrimagnetic ground state. Although in previous work we have used GGA + U corrections to describe both d [26] and f [27] valence electrons, due to the exploratory nature of this work we decided not to extend the current model beyond standard GGA. The effect of on-site Hubbard-type interactions on the values of the exchange integrals has recently been discussed elsewhere [28].

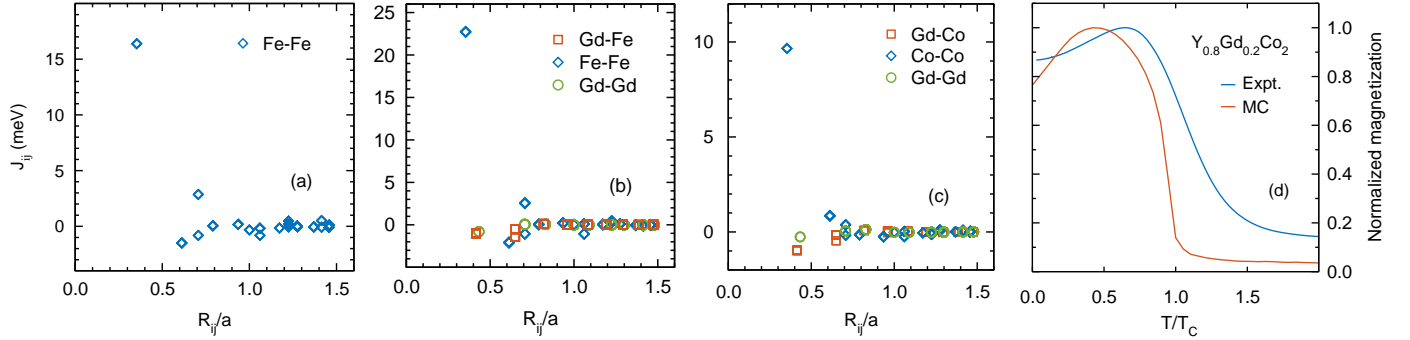


Figure 4: Exchange integrals as a function of normalized interatomic distance calculated using SPR-KKR for (a) YFe₂, (b) GdFe₂, and (c) GdCo₂. For YFe₂ the moment on Y is fixed at zero, so only the Fe-Fe exchange integrals are shown. (d) Normalized magnetization as a function of normalized temperature for Y_{0.8}Gd_{0.2}Co₂. Monte Carlo *versus* experimental (zero-field cooled) results taken from Ref. [13].

Table 1: Atomic coordinates of the considered YFe₂, YCo₂, GdFe₂, and GdCo₂ Laves phases, space group $Fd\bar{3}m$ (no. 227), origin choice two.

atom	site	x	y	z
Y/Gd	$8a$	1/8	1/8	1/8
Fe/Co	$16d$	1/2	1/2	1/2

For Monte Carlo simulations of the Heisenberg Hamiltonian we used the Uppsala atomistic spin dynamics (UppASD) code [29, 30]. The simulated system consisted of ~ 13000 atoms with periodic boundary conditions. The radius of the exchange integrals cutoff sphere in the Heisenberg Hamiltonian was set to 1.5 lattice parameters. The exchange integrals were assumed to be temperature independent in the MC simulations. The simulations were performed using classical (Boltzmann) statistics, but it is worth noting that it has recently been possible to use quantum (Bose-Einstein) statistics using the UppASD code [31]. The magnetic moment on Y, since it is induced and expected to vanish with temperature, was set equal to zero in the MC simulations (first-principles calculations gave a moment of $\sim 0.5 \mu_B$). In the MC simulations, we used exchange integrals calculated with respect to the ferromagnetic ground state. We justify this on the grounds that MC simulations of GdCo₂ with exchange integrals obtained with respect to the paramagnetic ground state have yielded that material to be a paramagnet. This can be explained by the fact that the Co sublattice is metamagnetic in GdCo₂ [32].

Experimental lattice parameters were used to model the boundary compositions YFe₂ (7.36), YCo₂ (7.22), GdFe₂ (7.38), and GdCo₂ (7.24 Å) [7, 33]. For intermediate Y_{1-x}Gd_x(Fe_{1-y}Co_y)₂ concentrations, we assumed a linear behavior of the lattice parameters. The full range of Co and Gd concentrations were prepared with a step of 0.1, leading to a total of 121 cases considered (11 \times 11). The space group and atomic positions of the C15 Laves phase are shown in Table 1. The picture of the unit cell, generated using the VESTA code [34], is shown in Fig. 1.

3. Results and Discussion

In Fig. 3 we presents a Curie temperature dependence of Gd and Co concentrations for Y_{1-x}Gd_x(Fe_{1-y}Co_y)₂ determined from Monte Carlo simulations with parameters from first-principles calculations. For comparison, the four curves (red, green, blue, and yellow) are plotted based on experimental results [2, 3, 7–9]. Along the Co concentrations (y), our MC simulations preserve the characteristic Slater-Pauling behavior for $T_C(y)$. For Y_{1-x}Gd_xFe₂, we reproduce the linear behavior of the dependence of T_C on Gd concentration, please compare with the bottom panel of Fig. 2. Our T_C estimates agree relatively well with experimental results in all boundary regions except for the YCo₂ neighborhood. The reason for the observed discrepancy is a combination of two factors: (a) the paramagnetic nature of the YCo₂ remaining on the verge of satisfying the Stoner criterion ($N(E_F)I \simeq 0.9$) [20, 32], and (b) the previously raised problem of GGA’s failure to correctly describe the magnetic ground state of Co [18]. Leaving aside the overestimation of the results near YCo₂, the map obtained for a system containing three magnetic elements shows that a realistic first-principles T_C analysis for complex magnetic materials is possible allowing, for example, to determine the concentrations of the individual components leading to a specific T_C value, e.g. 300 K, as sought for magnetocaloric materials for use in magnetic coolers.

T_C values were estimated from magnetic moments and exchange integrals calculated from first principles. Figure 4 shows the calculated exchange integrals as a function of normalized interatomic distance for considered ferromagnetic boundary compositions. It is easy to see that in each case the dominant contribution to the Heisenberg Hamiltonian comes from first-neighbor interactions at the Fe/Co sites. We verified that restricting the MC simulation to this dominant exchange interaction would lead to an underestimation of the Curie temperature on the order of hundreds of kelvins compared to simulations that include other exchange integrals. The high values of first-neighbor Fe-Fe interactions observed in YFe₂, further increase in GdFe₂, as reflected by the linear increase in T_C

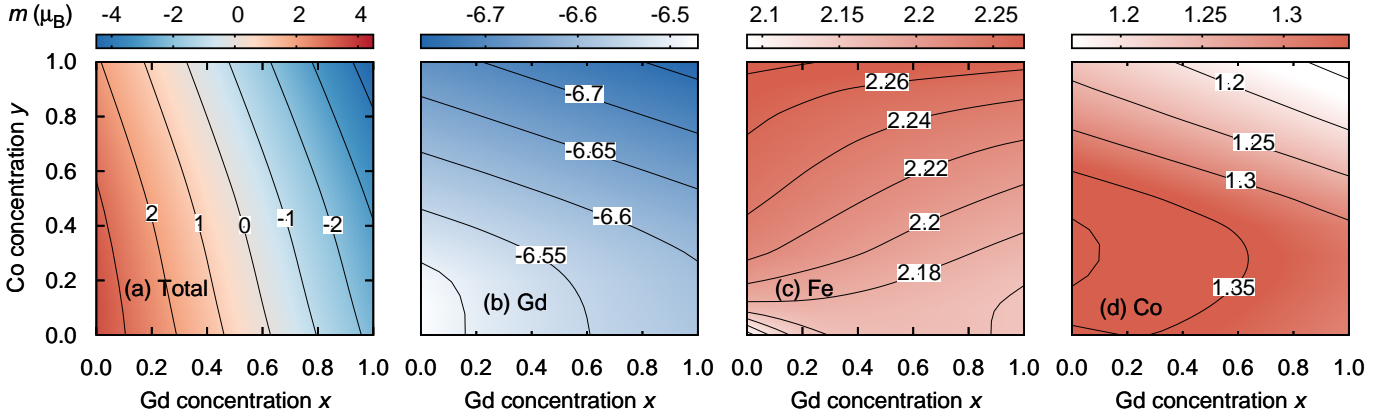


Figure 5: Magnetic moments in the ground state ($T = 0$ K) for the $Y_{1-x}Gd_x(Fe_{1-y}Co_y)_2$ system calculated using the SPR-KKR code.

observed with increasing Gd concentration in $Y_{1-x}Gd_xFe_2$ alloys, compare with Fig. 3 and the bottom panel of Fig. 2. Similar conclusions can be drawn from the comparison of Fe-Fe and Co-Co first-neighbor interactions for Gd compounds.

In addition to the values of exchange interactions just discussed, the second factor that significantly affects the T_C values obtained are the magnetic moments. Figure 5 presents the calculated magnetic moments in the ground state ($T = 0$ K) for the $Y_{1-x}Gd_x(Fe_{1-y}Co_y)_2$ system. While the atom-resolved values of magnetic moments do not differ by more than $\sim 0.2 \mu_B$ with concentrations, the total magnetic moment varies from about $-4 \mu_B$ to $+4 \mu_B$. This range is due to the antiparallel alignment of moments at the Fe/Co and Gd sites. The calculated values of the magnetic moments are about 2.2 and $1.3 \mu_B$ for Fe and Co and about $-6.6 \mu_B$ for Gd. These results are in good agreement with our previous theoretical results for the systems $Y_{1-x}Gd_xCo_2$ [13] and $Y(Fe_{1-y}Co_y)_2$ [20]. The calculated total magnetic moments are also in good agreement with the experimental results for the systems $Y_{1-x}Gd_xCo_2$ [13] and $Y(Fe_{1-y}Co_y)_2$ [35]. Interestingly, for certain concentrations we observe a zero total moment, implying a complete compensation of the opposite moments present on the different elements. We would like to recall that the results in the upper left corner of the magnetic moment map, describing the nearest neighborhood of YCo_2 , are incorrect because YCo_2 is in fact a magnetically disordered phase whose ground state is not correctly described in GGA.

For the positive (red) region of the total magnetic moment, due to the presence of uncompensated opposite magnetic moments, the relation $M(T)$ shows a positive slope at low temperatures, see Fig. 4(d). For the example $Y_{0.8}Gd_{0.2}Co_2$ concentration, our MC predicted increase in magnetization at low temperatures is confirmed by experimental (zero-field cooled) results [13]. For considered compounds with large positive total magnetic moment, we expect a large inverse magnetocaloric effect to occur in a region with positive $M(T)$ slope. The physics responsi-

ble for the shape of $M(T)$ curves can be understood by considering exchange integrals for different pairs of atoms. In Fig. 4 we see that the $4f-4f$ and $4f-3d$ interactions are much weaker than the $3d-3d$ interactions therefore the thermal disorder first affects the $4f$ sublattice, while the $3d$ sublattice remains (at least relatively) ordered, which means that the magnetic moments of the $4f$ sublattice no longer compensate, or compensate to a much lesser extent, the $3d$ moments, hence the initial increase in magnetization. For temperatures higher than the temperature for which the magnetization maximum occurs in Fig. 4(d), the simulated material begins to behave as a ferromagnet.

Figure 6 shows the valence band DOS for four stoichiometric compositions of the $Y_{1-x}Gd_x(Fe_{1-y}Co_y)_2$ system. All panels of Fig. 6 show results with spin polarization that is proportional to the values of calculated magnetic moments. As we said, the magnetic moments are about 2.2 , 1.3 , and $-6.6 \mu_B$ for Fe, Co, and Gd. In each case, the dominant contribution to the valence band comes from the $3d$ orbitals of the $3d$ elements (Fe and Co). For compounds with Gd, we observe an almost completely occupied one spin channel of the Gd $4f$ orbital and an almost empty second spin channel. The $4f$ bands are also much more localized than the $3d$ bands. The location of the occupied $4f$ bands is about -3.5 eV below the Fermi level. The difference in DOS between systems containing Co and Fe is mainly due to filling of the valence band with an extra electron for each Co atom relative to the Fe atoms. Similarly, as we mentioned earlier when discussing the results of Curie temperature calculations, the obtained ferromagnetic solution for YCo_2 should be treated with caution in view of the experimentally found paramagnetic ground state for this phase.

4. Summary and Conclusions

In this paper, we theoretically described the Curie temperature dependence of the $Y_{1-x}Gd_x(Fe_{1-y}Co_y)_2$ pseudobinary system using the combined Monte Carlo and first-

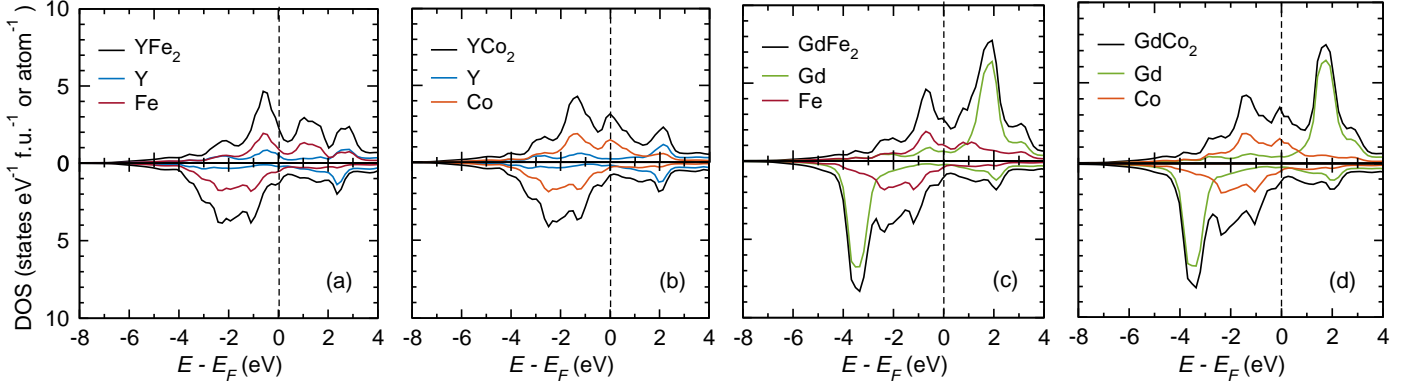


Figure 6: Densities of states (DOS) of YFe_2 , YCo_2 , GdFe_2 , and GdCo_2 as calculated with the SPR-KKR code.

principles methods. The calculation results agree well with the previous measurements except for the vicinity of the YCo_2 system. For the latter, instead of paramagnetic ground state, we obtained a ferromagnetic one. For the $\text{Y}_{1-x}\text{Gd}_x\text{Fe}_2$ subsystem we reproduced the linear dependence of T_C on Gd concentration, and for the $\text{Y}(\text{Fe}_{1-y}\text{Co}_y)_2$ and $\text{Gd}(\text{Fe}_{1-y}\text{Co}_y)_2$ subsystems we reproduced the characteristic Slater-Pauling-like dependence of T_C on concentration. The results presented here confirm the ability to efficiently predict Curie temperatures for magnetic systems containing up to three different magnetic elements simultaneously. Furthermore, the first-principles results show that the largest contribution to the Heisenberg Hamiltonian comes from Fe/Co nearest-neighbor exchange interactions. For the $\text{Y}_{1-x}\text{Gd}_x(\text{Fe}_{1-y}\text{Co}_y)_2$ system, we have also shown how the occurrence of a compensation point with an effective zero magnetic moment depends on the concentration of Co and Gd. In addition, using the example of the $\text{Y}_{0.8}\text{Gd}_{0.2}\text{Co}_2$ ferrimagnetic phase, we have shown that the model used allows to predict non-trivial magnetization-temperature dependence.

Acknowledgements

MW acknowledges the financial support of the National Science Centre Poland under the decision DEC-2018/30/E/ST3/00267. We acknowledge the financial support from the Foundation of Polish Science grant HOMING. The HOMING programme is co-financed by the European Union under the European Regional Development Fund. The computations were performed on resources provided by the Poznan Supercomputing and Networking Center (PSNC). We thank Pawel Leśniak and Daniel Depcik for compiling the scientific software and administration of the computing cluster at the Institute of Molecular Physics, Polish Academy of Sciences. We also thank Zbigniew Śniadecki for his comments and fruitful discussion.

References

- [1] F. Stein, M. Palm, G. Sauthoff, Structure and stability of Laves phases. Part I. Critical assessment of factors controlling Laves phase stability, *Intermetallics* 12 (7) (2004) 713–720. [doi:10.1016/j.intermet.2004.02.010](https://doi.org/10.1016/j.intermet.2004.02.010).
- [2] K. H. J. Buschow, R. P. van Stapele, Magnetic Properties of some Cubic Rare-Earth-Iron Compounds of the Type RFe_2 and $\text{R}_x\text{Y}_{1-x}\text{Fe}_2$, *J. Appl. Phys.* 41 (10) (1970) 4066–4069. [doi:10.1063/1.1658412](https://doi.org/10.1063/1.1658412).
- [3] A. T. Burkov, A. Y. Zyuzin, T. Nakama, K. Yagasaki, J. Schumann, H. Vinzelberg, Magnetotransport in $(\text{Y}_x\text{Gd}_{1-x})\text{Co}_2$ alloys near to magnetic phase boundary, *Phys. B Condens. Matter* 329–333 (2003) 543–544. [doi:10.1016/S0921-4526\(02\)02384-0](https://doi.org/10.1016/S0921-4526(02)02384-0).
- [4] Y. Yamada, H. Ohmae, NMR Study of $\text{Y}(\text{Fe}_{1-x}\text{Co}_x)_2$ and $\text{Zr}(\text{Fe}_{1-x}\text{Co}_x)_2$, *J. Phys. Soc. Jpn.* 48 (5) (1980) 1513–1518. [doi:10.1143/JPSJ.48.1513](https://doi.org/10.1143/JPSJ.48.1513).
- [5] T. Goto, T. Sakakibara, K. Murata, H. Komatsu, K. Fukamichi, Itinerant electron metamagnetism in YCo_2 and LuCo_2 , *J. Magn. Magn. Mater.* 90–91 (1990) 700–702. [doi:10.1016/S0304-8853\(10\)80256-2](https://doi.org/10.1016/S0304-8853(10)80256-2).
- [6] V. Paul-Boncour, O. Isnard, M. Guillot, A. Hoser, Metamagnetic transitions in $\text{Y}_{0.5}\text{Er}_{0.5}\text{Fe}_2\text{D}_{4.2}$ deuteride studied by high magnetic field and neutron diffraction experiments, *J. Magn. Magn. Mater.* 477 (2019) 356–365. [doi:10.1016/j.jmmm.2019.01.056](https://doi.org/10.1016/j.jmmm.2019.01.056).
- [7] P. Guzdek, J. Pszczoła, J. Chmíst, P. Stoch, A. Stoch, J. Suwalski, Electrical resistivity and Mössbauer effect studies of $\text{Y}(\text{Fe}_{1-x}\text{Co}_x)_2$ intermetallics, *J. Alloys Compd.* 520 (2012) 72–76. [doi:10.1016/j.jallcom.2011.12.081](https://doi.org/10.1016/j.jallcom.2011.12.081).
- [8] E. Burzo, D. P. Lazăr, L. Pali, Paramagnetic behaviour of $\text{Gd}(\text{Fe}_x\text{Co}_{1-x})_2$ compounds, *Phys. Status Solidi A* 45 (2) (1978) K145–K148. [doi:10.1002/pssa.2210450256](https://doi.org/10.1002/pssa.2210450256).
- [9] S. H. Kilcoyne, The evolution of magnetic correlations and onset of magnetic order in $\text{Y}(\text{Co}_{1-x}\text{Fe}_x)_2$, *Phys. B Condens. Matter* 276–278 (2000) 660–661. [doi:10.1016/S0921-4526\(99\)01731-7](https://doi.org/10.1016/S0921-4526(99)01731-7).
- [10] O. Isnard, V. Paul-Boncour, Z. Arnold, On the origin of the giant isotopic effect of hydrogen on the magnetic properties of $\text{YFe}_2\text{A}_{4.2}$ ($A = \text{H}, \text{D}$): A high pressure study, *Appl. Phys. Lett.* 102 (12) (2013) 122408. [doi:10.1063/1.4798260](https://doi.org/10.1063/1.4798260).
- [11] V. Paul-Boncour, M. Guillot, O. Isnard, A. Hoser, High field induced magnetic transitions in the $\text{Y}_{0.7}\text{Er}_{0.3}\text{Fe}_2\text{D}_{4.2}$ deuteride, *Phys. Rev. B* 96 (10) (2017) 104440. [doi:10.1103/PhysRevB.96.104440](https://doi.org/10.1103/PhysRevB.96.104440).
- [12] P. Kumar, A. Kashyap, B. Balamurugan, J. E. Shield, D. J. Sellmyer, R. Skomski, Permanent magnetism of intermetallic compounds between light and heavy transition-metal elements, *J. Phys. Condens. Matter* 26 (6) (2014) 064209. [doi:10.1088/0953-8984/26/6/064209](https://doi.org/10.1088/0953-8984/26/6/064209).
- [13] N. Pierunek, Z. Śniadecki, M. Werwiński, B. Wasilewski, V. Franco, B. Idzikowski, Normal and inverse magnetocaloric

- effects in structurally disordered Laves phase $Y_{1-x}Gd_xCo_2$ ($0 < x < 1$) compounds, *J. Alloys Compd.* 702 (2017) 258–265. doi:10.1016/j.jallcom.2017.01.181.
- [14] A. T. Burkov, A. Y. Zyuzin, T. Nakama, K. Yagasaki, Thermopower of $(Y_{1-x}Gd_x)Co_2$ alloys in a vicinity of zero-temperature magnetic phase boundary, *J. Magn. Magn. Mater.* 272–276 (2004) E1083–E1084. doi:10.1016/j.jmmm.2003.12.1118.
- [15] A. Burkov, T. Nakama, K. Yagasaki, Electronic Transport in Itinerant Metamagnets with Strong Static Disorder, *Solid State Phenom.* 168–169 (2011) 521–524. doi:10.4028/www.scientific.net/SSP.168-169.521.
- [16] K. A. Gschneidner Jr, V. K. Pecharsky, A. O. Tsokol, Recent developments in magnetocaloric materials, *Rep. Prog. Phys.* 68 (6) (2005) 1479–1539. doi:10.1088/0034-4885/68/6/R04.
- [17] Z. Śniadecki, M. Werwiński, A. Szajek, U. K. Röbler, B. Idzikowski, Induced magnetic ordering in alloyed compounds based on Pauli paramagnet YCo_2 , *J. Appl. Phys.* 115 (17) (2014) 17E129. doi:10.1063/1.4866848.
- [18] B. Wasilewski, W. Marciniak, M. Werwiński, Curie temperature study of $Y(Fe_{1-x}Co_x)_2$ and $Zr(Fe_{1-x}Co_x)_2$ systems using mean field theory and Monte Carlo method, *J. Phys. Appl. Phys.* 51 (17) (2018) 175001. doi:10.1088/1361-6463/aab75b.
- [19] Z. Śniadecki, N. Pierunek, B. Idzikowski, B. Wasilewski, M. Werwiński, U. K. Röbler, Y. Ivanisenko, Influence of structural disorder on the magnetic properties and electronic structure of YCo_2 , *Phys. Rev. B* 98 (9) (2018) 094418. doi:10.1103/PhysRevB.98.094418.
- [20] B. Wasilewski, Z. Śniadecki, M. Werwiński, N. Pierunek, J. Rusz, O. Eriksson, Electronic specific heat coefficient and magnetic properties of $Y(Fe_{1-x}Co_x)_2$ Laves phases: A combined experimental and first-principles study, *Phys. Rev. B* 100 (13) (2019) 134436. doi:10.1103/PhysRevB.100.134436.
- [21] H. Ebert et al., The Munich SPR-KKR Package, Version 7.7 <http://ebert.cup.uni-muenchen.de/SPRKKR>.
- [22] H. Ebert, D. Ködderitzsch, J. Minár, Calculating condensed matter properties using the KKR-Green's function method—recent developments and applications, *Rep. Prog. Phys.* 74 (9) (2011) 096501. doi:10.1088/0034-4885/74/9/096501.
- [23] J. P. Perdew, K. Burke, M. Ernzerhof, Generalized gradient approximation made simple, *Phys. Rev. Lett.* 77 (18) (1996) 3865–3868. doi:10.1103/PhysRevLett.77.3865.
- [24] P. Soven, Coherent-potential model of substitutional disordered alloys, *Phys. Rev.* 156 (3) (1967) 809–813.
- [25] A. I. Liechtenstein, M. I. Katsnelson, V. A. Gubanov, Exchange interactions and spin-wave stiffness in ferromagnetic metals, *J. Phys. F Met. Phys.* 14 (7) (1984) L125. doi:10.1088/0305-4608/14/7/007.
- [26] J. Skoryna, S. Pacanowski, A. Marczyńska, M. Werwiński, A. Rogowska, M. Wachowiak, Ł. Majchrzycki, R. Czajka, L. Smardz, XPS valence band studies of nanocrystalline $ZrPd$ alloy thin films, *Surf. Coat. Technol.* 303 (2016) 125–130. doi:10.1016/j.surfcoat.2016.03.030.
- [27] J. A. Morkowski, G. Chelkowska, M. Werwiński, A. Szajek, R. Troć, C. Neise, X-ray photoemission spectrum, electronic structure, and magnetism of UCu_2Si_2 , *J. Alloys Compd.* 509 (25) (2011) 6994–6998. doi:10.1016/j.jallcom.2011.04.026.
- [28] S. Keshavarz, I. Di Marco, D. Thonig, L. Chioncel, O. Eriksson, Y. O. Kvashnin, Magnetic two-dimensional electron liquid at the surface of Heusler semiconductors, *Phys. Rev. Mater.* 4 (2) (2020) 021401. doi:10.1103/PhysRevMaterials.4.021401.
- [29] B. Skubic, J. Hellsvik, L. Nordström, O. Eriksson, A method for atomistic spin dynamics simulations: Implementation and examples, *J. Phys. Condens. Matter* 20 (31) (2008) 315203. doi:10.1088/0953-8984/20/31/315203.
- [30] O. Eriksson, A. Bergman, L. Bergqvist, J. Hellsvik, *Atomistic Spin Dynamics: Foundations and Applications*, Oxford University Press, 2017.
- [31] L. Bergqvist, A. Bergman, Realistic finite temperature simulations of magnetic systems using quantum statistics, *Phys. Rev. Mater.* 2 (1) (2018) 013802. doi:10.1103/PhysRevMaterials.2.013802.
- [32] E. Gratz, A. S. Markosyan, Physical properties of RCo_2 Laves phases, *J. Phys. Condens. Matter* 13 (23) (2001) R385. doi:10.1088/0953-8984/13/23/202.
- [33] H. Oesterreicher, W. E. Wallace, Studies of pseudo-binary laves-phase systems containing lanthanides: I. Constitution and magnetic properties of the $GdAl_2$ - $GdFe_2$, $GdAl_2$ - $GdCo_2$ and $ErCo_2$ - $ErAl_2$ systems, *J. Common Met.* 13 (1) (1967) 91–102. doi:10.1016/0022-5088(67)90050-1.
- [34] K. Momma, F. Izumi, *VESTA* : A three-dimensional visualization system for electronic and structural analysis, *J. Appl. Crystallogr.* 41 (3) (2008) 653–658. doi:10.1107/S0021889808012016.
- [35] A. R. Piercy, K. N. R. Taylor, Evidence for an itinerant electron moment in cubic Laves-phase rare-earth - transition-metal compounds, *J. Phys. C: Solid State Phys.* 1 (4) (1968) 1112. doi:10.1088/0022-3719/1/4/330.